

Relationship Between Aquifer Processes and Groundwater Quality: A Case of Olbanita Aquifer System, Lower Baringo Basin, Kenya Rift

Authors: Sosi, Benjamin, Getabu, Albert, Maobe, Samson, and Barongo, Justus

Source: Air, Soil and Water Research, 12(1)

Published By: SAGE Publishing

URL: <https://doi.org/10.1177/1178622119889910>

BioOne Complete (complete.BioOne.org) is a full-text database of 200 subscribed and open-access titles in the biological, ecological, and environmental sciences published by nonprofit societies, associations, museums, institutions, and presses.

Your use of this PDF, the BioOne Complete website, and all posted and associated content indicates your acceptance of BioOne's Terms of Use, available at www.bioone.org/terms-of-use.


Usage of BioOne Complete content is strictly limited to personal, educational, and non - commercial use. Commercial inquiries or rights and permissions requests should be directed to the individual publisher as copyright holder.

BioOne sees sustainable scholarly publishing as an inherently collaborative enterprise connecting authors, nonprofit publishers, academic institutions, research libraries, and research funders in the common goal of maximizing access to critical research.

Relationship Between Aquifer Processes and Groundwater Quality: A Case of Olbanita Aquifer System, Lower Baringo Basin, Kenya Rift

Air, Soil and Water Research
Volume 12: 1–12
© The Author(s) 2019
Article reuse guidelines:
sagepub.com/journals-permissions
DOI: 10.1177/1178622119889910



Benjamin Sosi^{1,2} , Albert Getabu², Samson Maobe²
and Justus Barongo³

¹Department of Natural Resources, Egerton University, Nakuru, Kenya. ²Department of Natural Resources, Kisii University, Kisii, Kenya. ³Department of Geology, University of Nairobi, Nairobi, Kenya.

ABSTRACT: A hydrogeochemical relation has been hypothesized through the analyses of physiochemical data of a fractured volcanic rock aquifer located in the Lower Baringo Basin, Kenyan Rift. Data sets included 15 individual metrics determined in 42 dry and wet season water samples obtained from 6 boreholes in the area. Aquifer evolutionary theory was postulated using sequential principal component analysis (PCA) and hierarchical cluster analysis. To eliminate the effects of scale dimensionality, PCA decomposed the variable data into 4 factors, namely, electrical conductivity, salinity, alkalinity, and carbonate equilibrium with external pH control for the dry season and salinity, carbonate equilibrium with external pH control, alkalinity, and electrical conductivity for the wet season. The main result depicted a major shift in the variability factor from electrolytic conductivity (34.8%) in the dry season to salinity (23.5%) in the wet season. Ward's linkage cluster analysis partitioned the aquifer into 2 spatially discrete associations; the western and the eastern entities, respectively, in spite of their shared recharge area. These agglomerative scheduling validated in an integrative approach (with groundwater flow predictions using a calibrated petrophysical groundwater model for the area) linked the 4 factors to aquifer processes and 3 pathways: fault permeability, weathering processes, and water-rock interaction. Statistical approaches are, therefore, useful in the conceptualization of pollutant sources and their attenuation for effective groundwater quality management.

KEYWORDS: Groundwater evolutionary processes, water quality characterization, Olbanita, Kenya Rift

RECEIVED: October 26, 2019. **ACCEPTED:** October 28, 2019.

TYPE: Original Research

FUNDING: The author(s) disclosed receipt of the following financial support for the research, authorship, and/or publication of this article: This research was funded by Kenya Government through the National Research Fund (website: <http://www.nrf.go.ke>), grant number NRF/R/2016/FORM-1A.

DECLARATION OF CONFLICTING INTERESTS: The author(s) declared no potential conflicts of interest with respect to the research, authorship, and/or publication of this article.

CORRESPONDING AUTHOR: Benjamin Sosi, Department of Natural Resources, Egerton University, Nakuru, Kenya, and Department of Natural Resources, Kisii University, Kisii, Kenya. Email: sosibenja@gmail.com

Introduction

Groundwater quality deterioration is a fundamental concern world over. Its quality characteristics in sub-Saharan Africa exhibit a wide spatial and temporal variability.^{1,2} The high volcanic fluoride (>1.5 mg/L) according to World Health Organization³ depicts widespread variability in groundwater aquifers of the African Rift.^{4,5} Continued urbanization is also rapidly causing increasingly poorer quality groundwater.^{1,2} However, the resource is strategically most reliable to exterminate the emergent demand.² Improved hydrochemical characterization of aquifers in such highly heterogeneous areas, decoupling the relation between groundwater quality and aquifer lithology, could enhance their effective management.^{6–8} Pazand⁹ observed that sustainable development and management of the quality of groundwater resources in arid and semi-arid lands is achievable through improved understanding of geochemical evolution and groundwater processes.

The determination of groundwater evolutionary processes concerning groundwater quality in fractured confined aquifers is complex. Large field experimental and geochemical laboratory data sets require proper management, elaboration, and interpretation tools and techniques.⁶ Güler et al¹⁰ noted that the interpretation of associations exclusively based on graphical techniques is fraught with difficulties owing to the simultaneous nature of aquifer processes and their effects. Recent studies by

Nwankwoala,¹¹ Pazand,⁹ Moghimi,¹² and Rotiroti et al⁶ established the value of multivariate techniques such as principal component analysis (PCA) and hierarchical clustering analysis (HCA) in the provision of quantitative measures of correlation between water quality parameters and fundamental aquifer processes. PCA is widely utilized to characterize groundwater pollution sources,⁹ while HCA is used to deduce spatial variability among sampling sites.¹³ An integrative application of PCA and HCA was employed by Rotiroti et al⁶ and Moghimi¹² to interpret processes affecting groundwater hydrochemistry and by Yidana et al,⁷ to evaluate evolutionary trends of groundwater dynamics and by Majeed et al¹⁴ to assess spatial patterns of pollutants in water. Several investigators^{15,16} utilized z-score or log conversions to normalize physical and chemical data acquired from groundwater sources. However, Everitt et al¹⁷ noted that such transformations could eliminate legitimate data values from the analysis. It is therefore suggested that Ward's Linkage agglomeration procedure could automatically rescale metric data into a range and yield good recovery of clusters.

Despite the significance of groundwater,² the reported high fluoride variability,^{4,5} and emergent urbanization^{1,2} in the region, knowledge on groundwater evolution and quality remain elusive. In this study, we postulate an evolutionary trend of a fractured volcanic aquifer based on multivariate statistics of groundwater quality data of the area. These joint hydrochemical evaluations of



Creative Commons Non Commercial CC BY-NC: This article is distributed under the terms of the Creative Commons Attribution-NonCommercial 4.0 License (<http://www.creativecommons.org/licenses/by-nc/4.0/>) which permits non-commercial use, reproduction and distribution of the work without further permission provided the original work is attributed as specified on the SAGE and Open Access pages (<https://us.sagepub.com/en-us/nam/open-access-at-sage>).

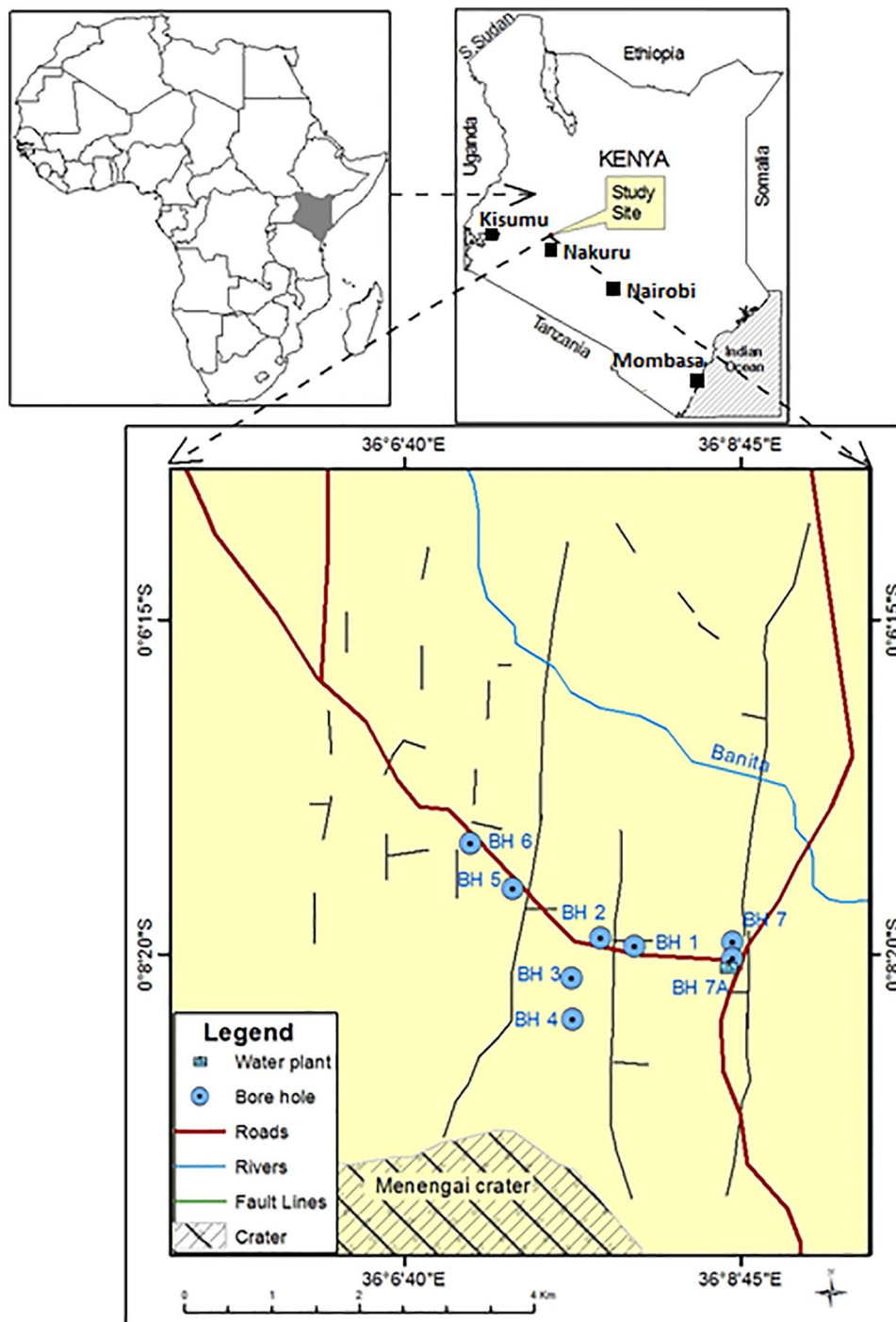


Figure 1. Location of Olbanita aquifer in Kenya showing sampled boreholes (blue circled dots).

relationships among deep groundwater wells and time-series groundwater quality variations are a fundamental step needed vis-à-vis variability in groundwater processes.

Materials and Methods

Study area

The Olbanita aquifer system is located in the lower Baringo basin of the Kenyan Rift (Figure 1). It is characterized by proximity to the equator and by its elevation which ranges from 1750 meters to 1880 meters above sea level. According to

National Council for Population and Development,¹⁸ the demographic profile for Nakuru County (wherein the Olbanita aquifer system is located) in 2009 was 1 602 637 and is projected to increase to 2 400 367 in 2030 and 3 013 869 in 2050. The city of Nakuru, situated in the upper Lake Nakuru Basin in the south, relies heavily on the 8 wells drilled in the adjacent Lower Baringo basin for potable water supply. As noted by GOK,¹⁹ water availability problems in the greater Nakuru and Baringo basins had negatively impacted on resident communities and the regional gross domestic product. Within the city, where the abstracted water is used, high incidences of

diarrhoeal infections become significant within the overall disease burden.²⁰

The hydrogeology of the area comprises fractured and weathered volcanic rocks and lacustrine sediments. The weathered tuffs sandwiched between the Samburu basalts and the Wasagess flows (phonolites and trachytes) of the Rumuruti group form the best aquifers in Olbanita area. The near N-S trending fault systems interrupting the aquifer system at 5 sites provide groundwater high porosity pathways. At a regional semi-arid climate, the open-faulted drainage, together with the semi-arid climate, renders groundwater in the area indispensable for human subsistence. The confined aquifer in the area recharges from the high altitude areas of Bahati (east of the area) and Menengai, where ecological conditions permit households to grow coffee, tomato, and maize as high-value enterprises.

Sampling and analysis methods

The sampling design in this study involved 6 out of 8 sampling sites constituted of boreholes in the Olbanita aquifer system located in the Kenya Rift (Figure 1). The sampling sites were located using a Garmin GPSmap60CSx model. At each sampling site, 4 replicate samples were taken monthly in 250-mL high-density plastic bottles which had already been pre-cleaned by using concentrated nitric acid and drenched in deionized water. The samples were screened through Millipore membrane filters of pore size 0.2 micrometers to remove suspended solids. Thereafter, the water samples for sulfate analysis were precipitated using 0.2 M Zn(CH₃COO)₂ while samples for metal analysis were acidified in concentrated HCl or HCO₃⁻ 1 mL per 100 mL sample. In situ parameters (pH, electrical conductivity, and total dissolved solids) were measured using Hanna Instruments multiparameter meter model HI98194. Out of the 4 samples taken in plastic bottles, 2 replicate samples were stored in ice and taken to the laboratory for determination of geochemical parameters, namely Na⁺, K⁺, Ca²⁺, Cl⁻, F⁻, SO₄²⁻, H₂S, Total CO₂, CO₃²⁻, HCO₃⁻, H₂CO₃, and NH₄⁺. The concentrations of sulfate and chloride components in this study were quantified using ultraviolet-visible spectrophotometer model UV-1800 while the ions of Na, F, Ca, K, and NH₃ were quantified using an Ion-Selective Electrode (ISE) model ELIT 9801 as detailed by Victoria and the US Environmental Protection Agency (US EPA).²¹ Concentrations of nonionic components namely total carbonate carbon (TCC) and H₂S were quantified using titrimetric methods as also described in Victoria and the US EPA.²¹ Before ISE analysis, the acidified samples were re-digested using a strong alkali solution. TCC was further speciated into CO₃²⁻, CO₂, H₂CO₃, and HCO₃⁻.

To evaluate the appropriateness of geochemical data for factor analysis, Kaiser-Mayer-Olkin (KMO) measure of sampling adequacy and Bartlett's test of sphericity were performed.^{22,23} The KMO index was found to be 0.6 indicating a moderate degree of correlation among the variables could be appropriately carried out. In addition, Bartlett's test of sphericity was significant

(Bartlett $\chi^2 = .570$, 66 *df*, $P < .001$), confirming the suitability of factor analysis on the data collected in this study. The results of the assessment depict a lower number of variables (factors) that may be used to elucidate the variability in the hydrochemical data. The correlation matrix was further inspected for correlation coefficients greater than 0.3.²⁴ Statistically significant correlations in physical-chemical data sets for each season were identified through the application of the Spearman's rho for nonnormally distributed data. Most of the correlation coefficients are over 0.3 indicating that factor analysis may be utilized to provide significant reductions in data dimensionality. Helsel²⁵ and Rangeti et al²⁶ warn about the dangers of such simplified substitutions for nondetectable concentrations (by using numerical surrogates such as one-half the detection limit). Data were, therefore, automatically rescaled for HCA (because each predictor variable adopted a different scale of measurement), though exempted data sets for PCA. The laboratory geochemical data sets were utilized for PCA considering that the bottom-line correlation matrix (based on the Spearman rank) has the effect of standardizing the variable data.²⁷ Therefore, it is a more robust estimation technique that is less responsive to outliers compared with the widely used Pearson correlation matrix.²⁷

Groundwater quality data were further subjected to PCA and HCA. All statistical computations were executed using MS Excel spreadsheet and SPSS software version 20.0. For the PCA matrix, orthogonalization of factors was based on the rotated varimax method (with significant eigenvalue loadings $> \pm 0.5$) and a derived scree plot (with the criterion of eigenvalues > 1) was inspected for purposes of extracting varifactors.²⁸ For HCA, the software's algorithm utilized Euclidean distances and "sum of squared errors" to minimize the criterion function.

Results and Discussion

General consideration of data sets

Based on the test of skewness which uses the arithmetic mean and standard deviation, the physical-chemical parameters such as total dissolved solids (TDS), pH, electrical conductivity (EC), and the ions such as Cl⁻, Na⁺, F⁻, Ca²⁺, SO₄²⁻, H₂CO₃, CO₃²⁻, and H₂S are not considered to follow a normal frequency distribution²⁹ across the study area and between the sampling seasons. On the contrary, CO₂ and NH₄ depicted Gaussian distribution (ie, a significant departure from normality with a skew statistic > 2) (Table 1). The binomial nature of the former is an indication of natural substandard waters characterized by high mineralization. Supersaturation of Olbanita groundwater may be linked to processes like the dissolution of halide, ion exchange, and weathering of sodium-rich plagioclases (usually giving rise to clay mineralogy). The high concentration of H₂S is an indication of very deep circulation attaining anoxic conditions accompanied by abundant bacterial activity.

To offset the effects on mineral dissolution caused by dilution by meteoric waters from the analyses, seasonal data sets were analyzed independently. The initial step in the analysis

Table 1. Descriptive statistical data for all the parameters for the sampling period (n=6, N=42).

	N	STATISTIC	RANGE	MINIMUM	MAXIMUM	MEAN	SD	SKEWNESS	
								STATISTIC	SE
pH	42		1.670	7.400	9.070	8.16452	0.441495	0.105	0.365
TDS	42		156.000	242.000	398.000	320.16667	45.152272	-0.231	0.365
EC	42		312.000	482.000	794.000	641.80952	92.302324	-0.162	0.365
Cl	42		10.640	10.180	20.820	14.69536	2.686202	0.948	0.365
Na	42		127.420	134.320	261.740	173.22667	35.178236	1.232	0.365
SO ₄	42		19.890	0.900	20.790	7.85314	6.578745	0.705	0.365
F	42		9.580	3.230	12.810	6.36310	3.310061	0.804	0.365
Ca	42		15.190	2.150	17.340	6.40024	4.675027	1.659	0.365
K	42		11.500	1.970	13.470	6.56071	3.822435	0.284	0.365
CO ₂	42		168.206	134.404	302.610	230.40724	52.722064	-0.151	0.365
H ₂ CO ₃	42		28.816	0.758	29.574	8.04064	7.570068	1.358	0.365
HCO ₃	42		220.384	181.518	401.903	306.08954	69.488132	-0.118	0.365
CO ₃	42		33.031	0.490	33.522	5.42143	6.540314	2.469	0.365
H ₂ S	42		0.720	0.000	0.720	0.03374	0.109123	6.360	0.365
NH ₄	42		0.530	0.360	0.890	0.56310	0.159381	0.441	0.365
Valid N (listwise)	42								

Units: ppm (except for pH and EC. EC in $\mu\text{S/cm}$).

was to account for the extent of mutual variability between individual pairs of water quality variables during the separate seasons. The inter-item correlation matrix of the measured parameters during the dry season and the wet season is provided in Tables 2 and 5, respectively.

Generally, the rotated component matrix was found to contain both positive and negative loadings (Tables 4 and 7). The work of Liu et al³⁰ as enumerated in Mohapatra et al³¹ observed that eigenvalue loadings near ± 1 designate a strong association between a variable and a principal component (PC); eigenvalues exceeding ± 0.75 represent strong correlation, eigenvalues between ± 0.5 and ± 0.74 represent moderate correlation and those approaching 0 depict weak correlations. Each PC was attributed to a process owing to which the corresponding variables are probably linearly linked. The underlying processes occurring within the aquifer as construed from the consequent eigenvalue loadings are presented in Tables 4 and 7 where significant eigenvalue loadings are indicated by using the * mark.

Dry season water quality parameters

For the dry season data, the pairs pH-F, TDS-EC, TDS-CO₂, TDS-HCO₃, EC-CO₂, EC-HCO₃, Cl-SO₄, Ca-K, Ca-NH₄, F-NH₄, CO₂-HCO₃, as well as HCO₃-CO₃ showed strongly significant relationships. The pairs pH-Na, pH-Ca, pH-H₂CO₃,

pH-NH₄, TDS-Na, EC-Na, K-Cl, Cl-CO₂, Cl-HCO₃, Na-F, Na-HCO₃, SO₄-CO₂, SO₄-HCO₃, Ca-F, NH₄-H₂CO₃, and HCO₃-H₂S depicted moderate correlations (Table 2).

Principal components extracted. Based on the eigenvalues > 1 criterion, 4 principal components explained variability in groundwater quality at the site (Figure 2). Based on the cumulative variance of the rotation sums of squared loadings of the dry season, the retained latent constructs account for 90.1% of the variance in the data set (Table 3). PC1 with the largest eigenvalue accounted for a maximum of the total variability (34.8%). PC 2 accounted for the total variation of 21%. The third PC explained 20.8% of the total variance, whereas final PC explained 13.6% of the remaining variation in the data. Observed eigenvalue decomposition corresponds to earlier observations by Hossain et al³² that after the first PC, the second PC explains the greatest of the residual variance and so forth.

The first principal component, PC1 (the conductivity component), is associated with significantly high concentrations of electrolytic ions indicated by TDS, EC, Na⁺, Cl⁻, SO₄²⁻, CO₂, and HCO₃⁻. TDS depicted a strong correlation with EC ($+0.99$, $\alpha=0.01$) due to the extensive range in the solubility of/and mineral diversity within the aquifer system. Under sluggish flow during the dry season, groundwater can attain chemical saturation regarding TDS. Statistical analyses

Table 2. Spearman rank correlation coefficients of the physicochemical parameters of groundwater for the dry season (November 2017–February 2018).

	PH	TDS	EC	CL ⁻	Na ⁺	SO ₄ ²⁻	F ⁻	Ca ²⁺	K ⁺	CO ₂	H ₂ CO ₃	HCO ₃ ⁻	CO ₃ ²⁻	H ₂ S	NH ₄ ⁺
pH	1.000	-.009	.067	-.156	.533**	-.003	.763**	-.525**	-.216	-.109	-.590**	.018	.611**	.161	-.683**
TDS	1.000	.985**	-.463*	-.463*	.702**	-.446*	.374	.278	-.017	.813**	.226	.756**	-.015	-.373	.147
EC	1.000	1.000	.985**	-.459*	.735**	-.404	.430*	.247	-.031	.779**	.182	.756**	.034	-.341	.098
Cl ⁻	1.000	1.000	1.000	1.000	-.373	.842**	-.200	.288	.526**	-.676**	.230	-.692**	-.371	.383	.037
Na ⁺	1.000	1.000	1.000	1.000	1.000	-.400	.679**	-.065	-.018	.499*	-.151	.549**	.298	-.221	-.233
SO ₄ ²⁻	1.000	1.000	1.000	1.000	1.000	1.000	.010	.134	.297	-.714**	.093	-.687**	-.225	.437*	-.223
F ⁻	1.000	1.000	1.000	1.000	1.000	1.000	1.000	-.546**	-.425*	.106	-.337	.202	.416*	-.004	-.752**
Ca ²⁺	1.000	1.000	1.000	1.000	1.000	1.000	1.000	1.000	.820**	.203	.472*	.126	-.424*	-.072	.774**
K ⁺	1.000	1.000	1.000	1.000	1.000	1.000	1.000	1.000	1.000	1.000	.294	-.235	-.314	.082	.513*
CO ₂	1.000	1.000	1.000	1.000	1.000	1.000	1.000	1.000	1.000	1.000	1.000	.929**	.120	-.486*	.331
H ₂ CO ₃	1.000	1.000	1.000	1.000	1.000	1.000	1.000	1.000	1.000	1.000	1.000	.063	-.966**	-.358	.545**
HCO ₃ ⁻	1.000	1.000	1.000	1.000	1.000	1.000	1.000	1.000	1.000	1.000	1.000	1.000	.149	-.593**	.273
CO ₃ ²⁻	1.000	1.000	1.000	1.000	1.000	1.000	1.000	1.000	1.000	1.000	1.000	1.000	1.000	.239	-.492*
H ₂ S	1.000	1.000	1.000	1.000	1.000	1.000	1.000	1.000	1.000	1.000	1.000	1.000	1.000	1.000	-.235
NH ₄ ⁺	1.000	1.000	1.000	1.000	1.000	1.000	1.000	1.000	1.000	1.000	1.000	1.000	1.000	1.000	1.000

The strong correlations between variables are specified by coefficients in bold fonts.

*Correlation is significant at $\alpha = 0.05$ level (2-tailed).

**Correlation is significant at $\alpha = 0.01$ level (2-tailed).

associate Na^+ with the dissolution or chemical weathering of sodium-rich plagioclases (to produce clay minerals) or the dissolution of halide.¹² The moderate correlation observed between Na and F (+0.7) and Ca-F (-0.5) coupled with a relatively weak association between the pairs; Na-Cl (-0.4) supports partial derivation of electrolytic ions from weathering of Na-rich feldspathic rocks, dissolution of accessory mineral apatite as well as carbonate materials as opposed to dissolution of either halide rocks. The insoluble products of rock weathering such as Cl^- and SO_4^{2-} show a strong positive correlation (+0.84, $\alpha=0.01$) but cumulatively tend to inhibit the electrical conductivity of groundwater. Within the hydrogeological framework, the pattern and, therefore, the provenance of weathering can be accounted for by the roughly N-S fracture-fissure zones (Figure 1).

The second principal component, PC 2 (the salinity component), is depicted mainly by Cl^- , SO_4^{2-} , Ca^{2+} , and K^+ ions in water. The anomalous distribution of Cl^- , SO_4^{2-} , and Ca^{2+} is attributable to ion exchange mechanisms in saturated aquifer zones. The relatively strong association between the pairs Cl- SO_4 (+0.8), and the moderate association between the pairs Ca-F, K-Cl, SO_4 - CO_2 , Cl- HCO_3 , and SO_4 - HCO_3 , indicate that aquifer water salinity is chiefly attributed to geologic derivation. In addition, agriculture is equally a major pollution source

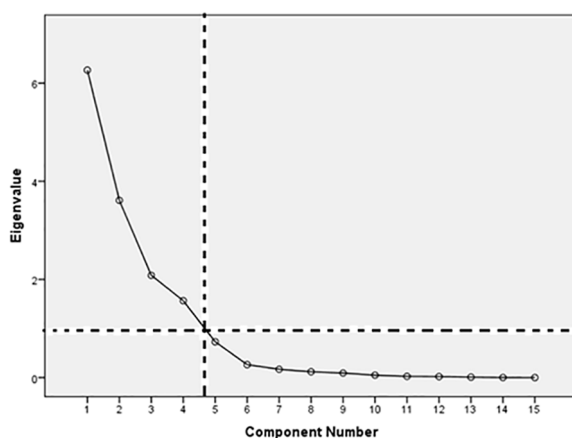


Figure 2. Cattell scree plot with eigenvalues > 1 criteria.

owing to the skewed distribution of Ca^{2+} which depicts strong correlations with K^+ ions (+0.8) and NH_4^- (+0.8) at $\alpha=0.01$.

The third principal component, PC 3, is the alkalinity component indicated by pH, and Na^+ , F^- , H_2CO_3 , and NH_4^- . The pH, Na, and F have positive loadings, whereas H_2CO_3 and NH_3 have moderate negative loading on this PC. H_2CO_3 and NH_3 are slightly broken down (ie, at about 25°C) to release H^+ , HCO_3^- , CO_3^{2-} , and NH_4^- thereby reducing the pH. Reduced pH significantly increases the rates of weathering introducing more Na and F from geologic sources.

The fourth PC represents carbonate equilibrium with exogenic pH control. The external factor controlling pH is H_2S . Sulfide in borehole waters is probably due to inorganic and bacterial changes in the deep aquifer under low dissolved oxygen, optimum growth range in pH (between 5.5 and 8.5) and optimum temperature (between 24°C and 42°C). Besides the authigenic derivation, meteoric waters may also leach agricultural SO_4^{2-} which may also undergo reduction at depth to sulfides.³³ Unfortunately, the latter may effectively be ruled out due to a complete lack of strong correlation neither with sulfide nor with ammonia (Table 2). Deeper depths within the bedrock are readily flushed by low mobility, oxygen-deficient groundwater; effects that are conditioned by low permeability at depth. The sulfate-reducing bacteria, *Desulfovibrio desulfuricans* obtain energy via the interconversion between sulfates and sulfides within the larger sulfur cycle in the aquifer system.^{34,35} Under these conditions, sulfates may be reduced to sulfides producing metallic sulfide which is again changed to H_2S under the action of H_2CO_3 . The dissociation of H_2CO_3 yields the CO_3^{2-} and donates H^+ which consequently reduces sulfates to sulfides.

Wet season water quality parameters

During the wet sampling season, the pairs pH-F, pH- H_2CO_3 , pH- CO_3 , TDS-EC, Na-F, F- H_2CO_3 , F- CO_3 , CO_2 - H_2CO_3 , and H_2CO_3 - CO_3 showed strong positive correlations at $\alpha=0.01$ (Table 5). The pairs pH-Na, pH- NH_3 , TDS-Cl, TDS-Na, TDS-F, EC-Cl, EC-Na, Cl-Na, K-Cl, Na- CO_3 , SO_4 - CO_2 , SO_4 - HCO_3 , SO_4 - H_2S , Ca-F, Ca- CO_2 , and Ca- NH_4 depicted moderate correlations at $\alpha=0.01$.

Table 3. Total variance explained for the dry season data.

COMPONENT	INITIAL EIGENVALUES			EXTRACTION SUMS OF SQUARED LOADINGS			ROTATION SUMS OF SQUARED LOADINGS		
	TOTAL	% OF VARIANCE	CUMULATIVE %	TOTAL	% OF VARIANCE	CUMULATIVE %	TOTAL	% OF VARIANCE	CUMULATIVE %
1	6.265	41.763	41.763	6.265	41.763	41.763	5.226	34.842	34.842
2	3.611	24.077	65.840	3.611	24.077	65.840	3.143	20.955	55.797
3	2.082	13.882	79.722	2.082	13.882	79.722	3.117	20.783	76.580
4	1.565	10.434	90.156	1.565	10.434	90.156	2.036	13.576	90.156

Table 4. Extracted factor loadings of the measured parameters during the dry season which suited the provisions of orthogonal varimax rotation.

	COMPONENT				COMMUNALITIES
	1	2	3	4	EXTRACTION
pH	0.037	-0.230	0.885*	0.087	0.844
TDS	0.968*	-0.112	0.091	-0.003	0.957
EC	0.959*	-0.083	0.156	0.012	0.952
Cl ⁻	-0.583*	0.763*	-0.126	-0.132	0.955
Na ⁺	0.725*	0.094	0.613*	-0.104	0.921
SO ₄ ²⁻	-0.548*	0.775*	0.086	-0.111	0.920
F ⁻	0.373	-0.053	0.897*	-0.056	0.950
Ca ²⁺	-0.205	0.889*	-0.299	-0.022	0.923
K ⁺	0.134	0.870*	-0.234	-0.183	0.862
CO ₂	0.952*	-0.174	-0.111	0.111	0.961
H ₂ CO ₃	0.219	0.204	-0.555*	-0.543	0.693
HCO ₃ ⁻	0.943*	-0.184	-0.077	0.056	0.932
CO ₃ ²⁻	0.139	-0.168	0.254	0.904*	0.930
H ₂ S	0.063	-0.045	-0.185	0.902*	0.854
NH ₄ ⁺	0.370	0.440	-0.728*	-0.094	0.869
Probable process	Electrical conductivity	Water salinity	Water alkalinity	Carbonate equilibrium with exogenic pH control	

Note: Significant eigenvalue loadings are indicated by using the * mark.

Principal components extracted. Based on the cumulative variance of the rotation sums of squared loadings of the wet season, the retained latent constructs account for 91.1% of the variability of the data set (Table 6).

PC1 with the largest eigenvalue accounted for the maximum of the total variability (23.5%). PC 2 accounted for the total variation of 22.8% and corresponds in concept to the first PC. The third and fourth PCs explained 22.8% and 22% of the total variance, respectively. Cattell's scree test plot is presented in Figure 2.

The first principal component, PC1 (the salinity component), is depicted mainly by K⁺, Ca²⁺, Cl⁻, SO₄²⁻, H₂S, and NH₄⁺ ions in water. As the component explains the largest variance in the data, it can be inferred that the groundwater in the study area is mainly saline. As nearly all carbonate ions depict a negative correlation in explaining PC1 and the non-carbonate alkali exceeds 50% in all (except BH7) boreholes (Figure 3), it can be deduced that NaCl constitutes the primary salinity at Olbanita. Abnormal distribution of Ca²⁺ and SO₄²⁻ may be characteristically associated with the ion exchange mechanisms in saturated aquifer zones. At the wet season pH, for instance, the monovalent Na⁺ is depleted from groundwater as it substitutes for divalent Ca²⁺ on exchangeable micro-pore surface water interfaces (Table 7). This

inference is demonstrated by BH 7 where none of the cation or anion pairs exceed 50% setting forth a secondary salinity characterized by Ca-Mg-SO₄ and/or chloride mixed type waters (Figure 3). The ions SO₄²⁻ and H₂S depict a strong positive correlation (+0.8 at $\alpha=0.01$) indicating either geologic provenance, probably due to deep circulation of oxygen-saturated waters causing aerobic conditions (Table 5), or anthropogenic derivation, probably due to their simultaneous positive contribution to PC1 along with ammonia (Table 7). The moderate correlations within the pairs NH₃-Ca (+0.7) and NH₃-H₂CO₃ (+0.6) imply anthropogenic contributions to the pH controls on aquifer water salinity. During the wet season, decreases in H⁺ cause a reduction in the water concentrations of K⁺, Ca²⁺, and Cl⁻. Aquifer salinity, therefore, is chiefly a construct of water-rock interactions and to a lesser extent anthropogenic inputs.

The second principal component, PC 2, depicts carbonate equilibrium with external pH control. The external factors controlling pH are SO₄²⁻ and H₂S, which are strongly correlated (+ 0.8, $\alpha = 0.01$). Sulfate and sulfide transformations in borehole waters are invariably mediated by bacterial changes under anaerobic conditions. *D. desulfuricans* may also produce H₂S under conditions of the measured pH range (optimum growth range in pH is between 5.5 and 8.5) and

Table 5. Spearman rank correlation coefficients for physiochemical parameters of groundwater for the wet season (March-May 2018).

	PH	TDS	EC	CL ⁻	Na ⁺	SO ₄ ²⁻	F ⁻	Ca ²⁺	K ⁺	CO ₂	H ₂ CO ₃	HCO ₃	CO ₃ ²⁻	H ₂ S	NH ₄
pH	1.000	.010	-.007	-.239	.621**	.225	.873**	-.557*	-.161	-.317	-.980**	-.240	.978**	-.041	-.666**
TDS	1.000	1.000	.991**	-.636**	.704**	-.235	.258	.003	-.019	.231	.045	.287	.072	-.350	.134
EC	1.000	1.000	1.000	-.645**	.686**	-.226	.224	.015	-.011	.249	.067	.298	.053	-.319	.124
CL ⁻	1.000	1.000	1.000	1.000	-.600**	.538*	-.265	.112	.629**	-.406	.166	-.459	-.259	.575*	.272
Na ⁺	1.000	1.000	1.000	1.000	1.000	-.261	.788**	-.370	-.150	.119	-.542*	.193	.697**	-.433	-.280
SO ₄ ²⁻	1.000	1.000	1.000	1.000	1.000	1.000	.082	-.022	.534*	-.686**	-.335	-.699**	.108	.760**	-.081
F ⁻	1.000	1.000	1.000	1.000	1.000	1.000	1.000	-.705**	-.208	-.381	-.853**	-.309	.867**	-.169	-.581*
Ca ²⁺	1.000	1.000	1.000	1.000	1.000	1.000	1.000	1.000	.461	.598**	.558*	.556*	-.490*	.123	.656**
K ⁺	1.000	1.000	1.000	1.000	1.000	1.000	1.000	1.000	1.000	.012	.159	.007	-.106	.511*	.337
CO ₂	1.000	1.000	1.000	1.000	1.000	1.000	1.000	1.000	1.000	1.000	.418	.979**	-.189	-.385	.225
H ₂ CO ₃	1.000	1.000	1.000	1.000	1.000	1.000	1.000	1.000	1.000	1.000	1.000	.362	-.930**	-.068	.637**
HCO ₃	1.000	1.000	1.000	1.000	1.000	1.000	1.000	1.000	1.000	1.000	1.000	1.000	-.098	-.454	.181
CO ₃ ²⁻	1.000	1.000	1.000	1.000	1.000	1.000	1.000	1.000	1.000	1.000	1.000	1.000	1.000	-.143	-.579*
H ₂ S	1.000	1.000	1.000	1.000	1.000	1.000	1.000	1.000	1.000	1.000	1.000	1.000	1.000	1.000	.010
NH ₄	1.000	1.000	1.000	1.000	1.000	1.000	1.000	1.000	1.000	1.000	1.000	1.000	1.000	1.000	1.000

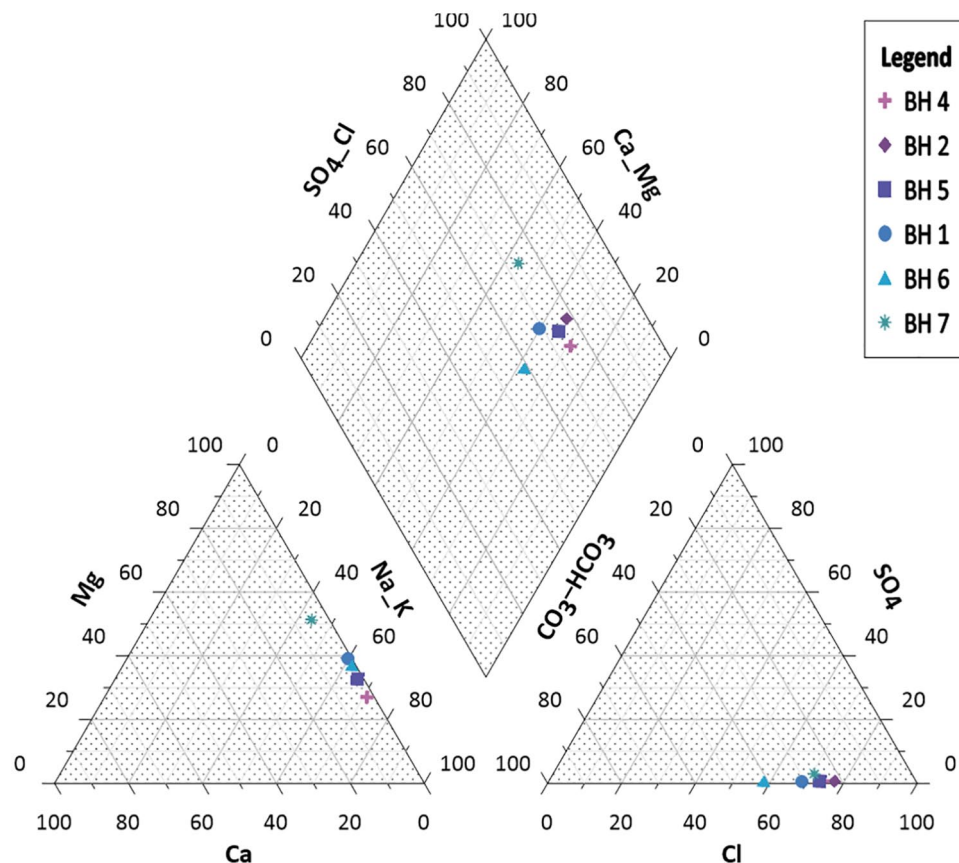
The strong correlations between variables are specified by coefficients in bold fonts.

*Correlation is significant at the .05 level (2-tailed).

**Correlation is significant at the .01 level (2-tailed).

Table 6. Cumulative variance explained for the wet season data.

COMPONENT	INITIAL EIGENVALUES			ROTATION SUMS OF SQUARED LOADINGS		
	TOTAL	% OF VARIANCE	CUMULATIVE %	TOTAL	% OF VARIANCE	CUMULATIVE %
1	5.691	37.938	37.938	3.519	23.460	23.460
2	4.423	29.489	67.427	3.427	22.844	46.304
3	2.273	15.154	82.581	3.420	22.799	69.103
4	1.278	8.521	91.102	3.300	21.999	91.102

**Figure 3.** Major composition in groundwater during the wet season.

optimum temperature between 24°C and 42°C. Under these conditions, sulfides (in the form of metal sulfide) undergo oxidation to sulfates which are again converted to H_2S under the action of H_2CO_3 . The dissociation of H_2CO_3 yields the ions CO_3^{2-} and H^+ which causes the reduction of sulfates to sulfides. Due to protracted mobility (diminutive residence period) of oxygen-saturated water in the wet season, reduced dissociation of H_2CO_3 yields less CO_3^{2-} and H^+ which consequently causes oxidation of sulfides to sulfates. BH 7 depicts the mixing effects probably conditioned by such pH shifts resulting from SO_4^{2-} and H_2S variability (Figure 3).

The third principal component, PC 3, is the alkalinity component as indicated by pH, CO_3^{2-} , H_2CO_3 , F^- and NH_4^- . The pH, CO_3^{2-} , and F^- have positive loading, whereas H_2CO_3 and NH_4^- have negative loading on this PC. The PC explains

the dissolution of fluoride through microbial activity releasing ammonia and thereby decreasing the pH. In addition, weak acids such as H_2CO_3 ionize sequentially releasing CO_3^{2-} , which again raises the pH of water.

The fourth PC is the electrolytic conductivity component which is associated with significantly high concentrations of electrolytic ions indicated by TDS, EC, Na^+ , and F^- . Statistical analyses (eg, Pazand⁹) associate F^- with weathering of the fluoro-apatite and silicate mineralogy, whereas Moghimi¹² linked Na^+ with the dissolution or weathering of sodium-rich plagioclases (clay mineralogy) or the dissolution of halide. The strong correlation observed between Na^+ and F^- (+0.9) and the weak association between Na^+ and Cl^- (-0.6) supports weathering plagioclase feldspars as the chief source as opposed to the dissolution of halide. Na and F ions

Table 7. The factor loadings of the measured parameters during the wet season which suited the provisions of orthogonal varimax rotation.

	COMPONENT				COMMONALITIES EXTRACTION
	1	2	3	4	
pH	-0.166	-0.169	0.948*	0.157	0.980
TDS	-0.148	0.292	0.060	0.934*	0.983
EC	-0.194	0.280	0.010	0.921*	0.964
Cl ⁻	0.830*	-0.292	-0.155	-0.379	0.942
Na ⁺	-0.071	-0.203	0.285	0.925*	0.983
SO ₄ ²⁻	0.694*	-0.702*	0.043	-0.059	0.980
F ⁻	-0.071	-0.246	0.735*	0.596*	0.961
Ca ²⁺	0.865*	0.002	-0.191	-0.307	0.879
K ⁺	0.929*	-0.040	-0.198	0.148	0.926
CO ₂	-0.088	0.967*	-0.147	0.092	0.974
H ₂ CO ₃	0.102	0.485	-0.762*	-0.023	0.827
HCO ₃ ⁻	-0.102	0.968*	-0.122	0.100	0.973
CO ₃ ²⁻	-0.118	0.237	0.944*	0.061	0.966
H ₂ S	0.572*	-0.503*	0.081	-0.237	0.643
NH ₄ ⁺	0.519*	0.367	-0.529*	-0.038	0.685
	Aquifer salinity	Carbonate equilibrium with external pH controls	Alkalinity of water	Electrolytic conduction	

Note: Significant eigenvalue loadings are indicated by using the * mark.

are the intrinsic constructs responsible for electrolytic conduction, as supported by their strong correlations with TDS. Within the hydrogeological framework, the pattern and, therefore, the provenance of weathering can be accounted for by the roughly N-S fracture-fissure zones. The component accounts for the lowest variability because of the reduced residence time of groundwater during the wet season exerting substantial reduction in TDS.

The dry to wet seasonal shift in variability from electrolytic conduction to low alkali salinity, respectively, is probably due to differential seasonal rates of weathering, flow and dilution processes in the aquifer. Significant correlations (at $\alpha = 0.01$) in the pairs Cl-SO₄, Ca-K, Ca-NH₃, F-NH₃, CO₂-HCO₃, HCO₃-CO₃, Na-F, and F-H₂CO₃ indicate that the water is alkaline to mildly acidic which are a manifestation of authigenic and to a lesser scale anthropogenic imprints. Key groundwater evolutionary trends suggest that silicate, carbonate, and/or accessory mineral apatite dissolution, as well as ion exchange at sorption sites with the clay-water interface, are the central sources of variability in the groundwater chemistry of the aquifer. Protracted mobility of oxygen-saturated water in the wet season, probably conditioned seasonal

by SO₄²⁻ and H₂S variability, though being an exogenic factor, restrained the pH constraint and hence carbonate equilibrium mixing reactions.

Spatial variability between sampling sites

The results of hierarchical clustering procedures were discrete clusters presented graphically in the form of a dendrogram by an averaging algorithm (Figure 4).

Based on rescaled Euclidean distances and the “sums of squared errors,” 2 main borehole clusters are conspicuous in the area. {Where to “prune” the tree (eg, using the continuous bold lines) is a vital factor in interpreting the results of the analysis. The within-cluster medium depict translational invariance in sample composition. Alternate shading was thus introduced to facilitate review}. The first cluster (forming the left-hand group) consists of the western zone cases (boreholes 2, 3, 4, 5 and 6), whereas the second cluster (forming the right-hand group) consists of the eastern zone borehole cases (boreholes 1, 7, and 7A). The former boreholes were deciphered to be hydraulically connected by a major inferred north west – south east fault which corresponds to a calibrated transmissivity-formation resistivity

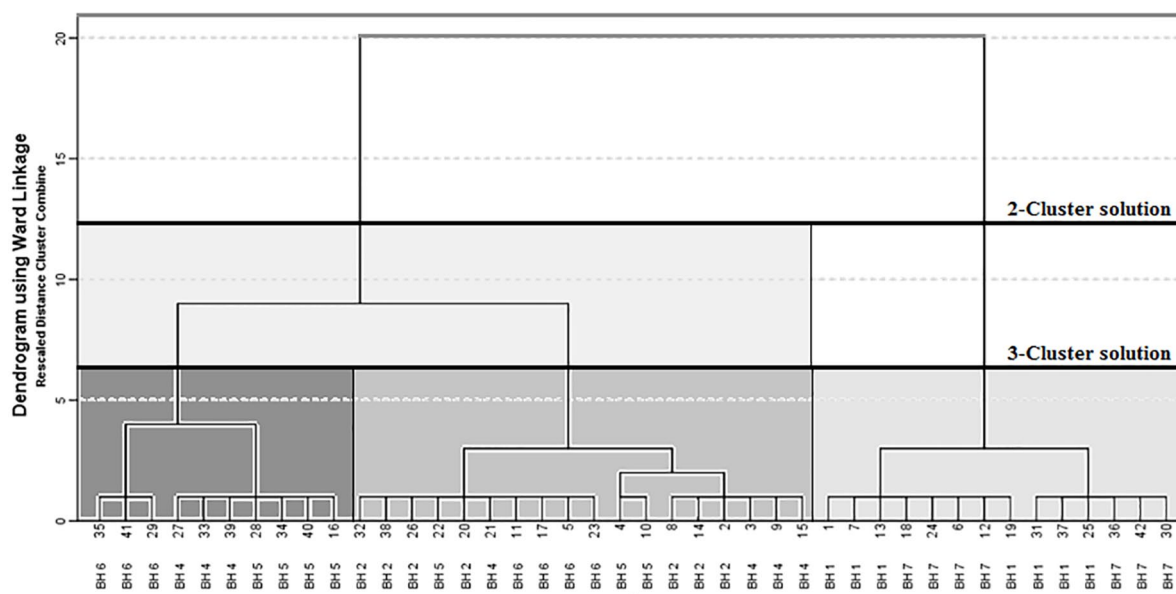


Figure 4. Dendrogram for clustering of groundwater sampling sites using the Euclidean distance metric (Ward's method).

model for the aquifer. Intrinsic permeability was empirically elevated along major fracture traces, consequently increasing yields of the affected boreholes. In addition, some wet season samples obtained from boreholes 4 (sample Nos. 27 and 33), 5 (sample Nos. 28, 34 and 40), and 6 (sample Nos. 29, 35 and 41) formed a mini-cluster within the former main group. The samples represent the effects of a high permeability fault/fracture structure which accentuates deep circulation of oxygen-saturated waters from recent precipitation events coupled with dilution within the corresponding season. We suggested low residence times of groundwater in the zone. Worth noting was the strong indication of low-carbonate alkali to mildly acidic mixed waters in the western zone at BH 6, which transits to become Ca-Mg sulfate and/or chloride water types of at BH 7 in the eastern periphery in the wet season.

The latter cluster contains boreholes located in the eastern compartment of the aquifer. Elevated values of Cl^- , SO_4^{2-} , and exceptionally low values of EC, TDS, pH, Na^+ , T-CO_2 , and HCO_3^- were recorded in these groundwater boreholes. However, values of EC, TDS, Ca^{2+} , SO_4^{2-} , and K^+ depicted an upward trend, whereas those of Na^+ , T-CO_2 , CO_3^{2-} , and HCO_3^- showed a downward trend from the dry season toward the wet season for these boreholes. By contrast, boreholes in the zone are not hydraulically connected via major fault structures. We, therefore, suggested that pore-level adsorption/desorption processes in which vast quantities of monovalent ions such as Na^+ and K^+ are removed from the groundwater in exchange for divalent ions control the observed variability in groundwater hydrochemistry in this zone. Lack of aquifer-scale hydraulic networks and the presence of clay micropores signify extended groundwater residence time favoring ion exchange reactions in the zone. Borehole 8 drilled in this zone dried-up after its completion because a clay layer was inadvertently targeted for production.

Conclusions

PCA and HCA are robust methods for establishing aquifer evolutionary structures. In this study, the PCA technique condensed multidimensional data into factors that explained seasonal variability in groundwater aquifer trends and quality. The dry to wet seasonal shift in variability from electrolytic conduction to salinity, respectively, is probably due to differential seasonal rates of weathering, flow, and dilution processes in the aquifer. The authors believe that key groundwater evolutionary trends, water-rock interactions, as well as ion exchange at sorption sites with the clay-water interface are the central restrictions of groundwater chemistry variability. HCA partitioned the aquifer into 2 discrete spatial associations, in spite of their indicated shared recharge area. These agglomerative scheduling validated in an integrative approach (with groundwater flow predictions using a calibrated petrophysical groundwater model for the area), linked each aquifer compartment to aquifer spatial heterogeneities and processes. The authors incontrovertibly deciphered groundwater residence periods for each compartment, diminutive for the western zone and protracted for the eastern zone. It is convincingly essential, therefore, based on pH shifts per season to design a groundwater quality monitoring plan and policy that reduces the number of measured parameters purposely to provide an opportunity cost in terms of resources for measurements elsewhere. A sustainable alternative would be to measure (as surrogates for the presence of the remaining parameters) EC during the dry season and K^+ , Ca^{2+} , and Cl^- during the wet seasons. The additional analyses may be required during extended dry periods accompanied by an upward trend in EC measurements.

Author Contributions

Conceptualization, B.S. and A.G.; methodology, B.S. and A.G.; software, B.S.; validation, B.S., A.G., S.M. and J.B.; formal analysis, B. S. and A.G.; investigation, B.S.; resources,

A.G., S.M. and J.B.; data curation, B.S. and A.G.; writing, B.S.; writing—review and editing, B.S., A.G., S. M., and J.B.; visualization, B.S. and A.G.; supervision, A.G., S.M., and J.B.; project administration, B.S. and S.M.; funding acquisition, A.G., S.M., and J.B.

Data availability

The data sets used and generated in this study are available upon request to sosibenjamin@yahoo.com.

ORCID iD

Benjamin Sosi  <https://orcid.org/0000-0001-6104-7011>

REFERENCES

- Nyika J, Onyari E. Hydrogeochemical analysis and spatial distribution of groundwater quality in roundhill landfill vicinity of South Africa. *Air Soil Water Res* 2019;12:1-8.
- Xu Y, Seward P, Gaye C, Lin L, Olago D. Preface: groundwater in sub-Saharan Africa. *Hydrogeol J* 2019;27:815-822.
- World Health Organization (WHO). *Guidelines for Drinking-Water Quality*. Geneva, Switzerland: WHO; 2011.
- Raj D, Shaji E. Fluoride contamination in groundwater resources of Alleppey, southern India. *Geosci Front* 2017;8:117-124.
- Olaka LA, Wilke FD, Olago DO, Odada EO, Mulch A, Musolff A. Groundwater fluoride enrichment in an active rift setting: Central Kenya Rift case study. *Sci Total Environ* 2016;545:641-653.
- Rotiroti M, Zanotti C, Fumagalli L, et al. Multivariate statistical analysis supporting the hydrochemical characterization of groundwater and surface water: a case study in northern Italy. *Rend Online Soc Geol Ital* 2019;47:90-96.
- Yidana SM, Bawoyobie P, Sakyi P, Fynn OF. Evolutionary analysis of groundwater flow: application of multivariate statistical analysis to hydrochemical data in the Densu Basin, Ghana. *J Afr Earth Sci* 2018;138:167-176.
- Ravikumar P, Somashekar RK. Principal component analysis and hydrochemical facies characterization to evaluate groundwater quality in Varahi river basin, Karnataka state, India. *Appl Water Sci* 2017;7:745-755.
- Pazand K. Geochemistry and multivariate statistical analysis for fluoride occurrence in groundwater in the Kuhbanan basin, Central Iran. *Mod Earth Syst Environm* 2016;2:72.
- Güler C, Thyne GD, Tağa H, Yıldırım Ü. Processes governing alkaline groundwater chemistry within a fractured rock (ophiolitic melange) aquifer underlying a seasonally inhabited headwater area in the Aladağlar range (Adana, Turkey). *Geofluids* 2017;2:1-21.
- Nwankwoala HO. Interpretation of hydro geochemical characteristics of deep aquifers in parts of Port Harcourt, Eastern Niger Delta. *Stand Sci Res Essays* 2013;1:154-163. <http://www.standresjournals.org/journals/SSRE>. Accessed February 16, 2018.
- Moghimi H. The study of processes affecting groundwater hydrochemistry by multivariate statistical analysis (case study: coastal aquifer of Ghaemshahr, NE-Iran). *Open J Geol* 2017;7:830-846.
- Esmaili S, Moghaddam AA, Barzegar R, Tziritis E. Multivariate statistics and hydrogeochemical modeling for source identification of major elements and heavy metals in the groundwater of Qareh-Ziaeddin plain, NW Iran. *Arab J Geosci* 2018;11: 5.
- Majeed S, Rashid S, Qadir A, Mackay C, Hayat F. Spatial patterns of pollutants in water of metropolitan drain in Lahore, Pakistan, using multivariate statistical techniques. *Environ Monit Assess* 2018;190: 128.
- Smeti EM, Golfinopoulos SK. Characterization of the quality of a surface water resource by multivariate statistical analysis. *Anal Lett* 2016;49:1032-1039.
- Cloutier V, Lefebvre R, Therrien R, Savard MM. Multivariate statistical analysis of geochemical data as indicative of the hydrogeochemical evolution of groundwater in a sedimentary rock aquifer system. *J Hydrol* 2008;353:294-313. doi:10.1016/j.jhydrol.2008.02.015.
- Everitt BS, Landau S, Leese M, Stahl D. Hierarchical clustering. *Cluster Anal* 2011;5:71-110.
- National Council for Population and Development (NCPD). *2015 Kenya National Adolescents and Youth Survey (NAYS)*. Nairobi, Kenya: NCPD; 2017.
- GOK. Rift valley water supply and sanitation project appraisal report. Working paper. Nakuru, Kenya: Rift Valley Water Services Board; 2004.
- Muchukuri E, Grenier FR. Social determinants of health and health inequities in Nakuru (Kenya). *Int J Equity Health* 2009;8: 16.
- Victoria E. Industrial waste resource guidelines sampling and analysis of waters, wastewaters, soils and wastes. *Environmental Protection Authority*. Victoria; 2009: 1-36.
- Voza D, Vuković M. The assessment and prediction of temporal variations in surface water quality—a case study. *Environ Monit Assess* 2018;190: 434.
- Joshi RR, Mulay P. Deep incremental statistical closeness factor-based algorithm DIS-CFBA; to assess diabetes mellitus. *Blood* 2018;115: 210.
- Tabachnick BG, Fidell LS. *Using Multivariate Statistics*. Boston, MA: Pearson Education; 2007.
- Helsel D. Much ado about next to nothing: incorporating nondetects in science. *Ann Occup Hyg* 2010;54:257-262. doi:10.1093/annhyg/mep092.
- Rangeti I, Dzwauro B, Barratt GJ, Otieno FA. Validity and errors in water quality data— a review. *Research and Practices in Water Quality*. Durban University of Technology, Durban, South Africa; 2015 September 9:95-112.
- US Department of Energy (US DOE). Multivariate statistical analysis of water chemistry in evaluating the origin of contamination in Many Devils Wash, Shiprock, New Mexico. https://www.energy.gov/sites/prod/files/S09257_ChemOrigin.pdf. Working paper S09257, Environmental Science Laboratory. Published 2012. Accessed February 16, 2018.
- Costello AB, Osborne JW. Practices in exploratory factor analysis: four recommendations for getting the most from your analysis. *Pract Assess Res Eval* 2005;10:1-9. <http://pareonline.net/getvn.asp?v=10&cn=7>. Accessed March 2, 2018.
- Kim HY. Statistical notes for clinical researchers: assessing normal distribution (2) using skewness and kurtosis. *Res Dentis Endodontics* 2013;38:52-54.
- Liu CW, Lin KH, Kuo YM. Application of factor analysis in the assessment of groundwater quality in a Blackfoot disease area in Taiwan. *Sci Total Environ* 2003;313:77-89.
- Mohapatra PK, Vijay R, Pujari PR, Sundaray SK, Mohanty BP. Determination of processes affecting groundwater quality in the coastal aquifer beneath Puri city, India: a multivariate statistical approach. *Water Sci Technol* 2011;64:809-817. doi:10.2166/wst.2011.605.
- Hossain M, Patras A, Barry-Ryan C, Martin-Diana A, Brunton N. Analysis of principal component analysis, hierarchical cluster analysis to classify different spices based on in vitro antioxidant activity and individual polyphenolic antioxidant compound. *J Funct Food* 2011;3:179-189.
- Tostevin R, Craw D, Van-Hale R, Vaughan M. Sources of environmental sulfur in the groundwater system, southern New Zealand. *Appl Geochem* 2016;1:1-6.
- Stanley W, Southam G. The effect of gram-positive (*Desulfosporosinus orientis*) and gram-negative (*Desulfovibrio desulfuricans*) sulfate-reducing bacteria on iron sulfide mineral precipitation. *Can J Microbiol* 2018;64:629-637.
- Anantharaman K, Brown CT, Hug LA, et al. Thousands of microbial genomes shed light on interconnected biogeochemical processes in an aquifer system. *Nat Commun* 2016; 7: 13219.